# Ferrocene-Containing ($\eta^6$-Hexamethylbenzene)ruthenium(II) Methoxycarbenes: Synthesis, Structure, and Electrochemistry

Petr Štěpnička* and Róbert Gyepes

*Department of Inorganic Chemistry, Charles University, Hlavova 2030, 12840 Prague, Czech Republic*

Olivier Lavastre and Pierre H. Dixneuf

*Chimie de Coordination et Catalyse, UMR 6509, CNRS, Université de Rennes I, Campus de Beaulieu, 35042 Rennes, France*

*Received June 9, 1997*[⊗]

The ($\eta^6$-hexamethylbenzene)dichlororuthenium(II) complexes [($\eta^6$-$C_6Me_6$)$RuCl_2$(L)], where L = $PMe_3$ (**1**), $PPh_3$ (**2**), $FcPPh_2$ (**3**; Fc = ferrocenyl), and Hdpf (**4**; Hdpf = ($\eta^5$-$C_5H_4PPh_2$)Fe($\eta^5$-$C_5H_4COOH$)), were reacted with terminal alkynes (FcC≡CH, $Me_3SiC$≡CH, and PhC≡CH) in the presence of $NaPF_6$ and methanol to give ($\eta^6$-hexamethylbenzene)chlororuthenium(II) methoxycarbenes [($\eta^6$-$C_6Me_6$)Ru(=C($OCH_3$)$CH_2$R)Cl(L)]$PF_6$ (L/R = $PMe_3$/Fc (**1a**), $PPh_3$/Fc (**2a**), $FcPPh_2$/Fc (**3a**), $FcPPh_2$/H (**3b**), $FcPPh_2$/Ph (**3c**), Hdpf/Fc (**4a**), Hdpf/H (**4b**), and Hdpf/Ph (**4c**)). All new compounds were characterized by NMR and IR spectroscopy and also studied by mass spectrometry in liquid matrix. The solid-state structure of **4a**·$CH_2Cl_2$ was determined by single-crystal X-ray diffraction. The electrochemical study of these bi- and trimetallic complexes displayed that upon oxidation, the Ru−ferrocenyl phosphine moiety undergoes a ferrocene/ferrocenium redox process followed by a Ru(II) → Ru(III) oxidation which is, however, markedly influenced by the preceding redox change. A redox dissymmetry of carbenes **1a**−**4c** was observed, as these exhibit communication within the Ru−phosphine part while the carbene ferrocenyl group remains isolated and practically unaffected.



## Introduction

Incorporating the redox-active ferrocenyl group(s) into an organometallic compound results in the formation of polymetallic species. Apart from being studied as the communicating redox systems,[1] such compounds exhibit unusual electrochemical activation of some molecules.[2] The conjugated ferrocene derivatives are being tested for second-[3] and third-order[4] optical nonlinearity with the aim of potential application in optical data storage and processing. The use of ferrocenyl ligands in organic synthesis and enantioselective catalysis is also well-documented.[5]

As described previously,[6] the presence of the ferrocenyl group in an arene−ruthenium(II) ferrocenyl(phenyl)allenylidene complex leads to mesomeric stabilization of this compound. In order to evaluate the mutual modification of the $Ru^{II}/Ru^{III}$ and the ferrocene/ferrocenium redox systems according to their possible communication, the ferrocene-containing ruthenium(II) carbenes of the general formula [($\eta^6$-arene)Ru(=C(OMe)$CH_2$R)(phosphine)Cl]$PF_6$ were studied. These compounds in which the ferrocenyl and $RuC_n$ ($n$ = 1) moieties are separated by the methylene group have not been studied yet. Generally, there are two simple ways to prepare ruthenium(II)−ferrocene oligometallic complexes of this type: (a) coordination of the ferrocenyl moiety containing phosphines to ruthenium, (b) transformation of terminal alkynes bearing the ferrocenyl group to carbene complexes. The phosphine complexes can be obtained by a reaction of the [($\eta^6$-arene)$RuCl_2$]$_2$ dimer and the corresponding phosphine. As for the preparation of carbene complexes, it has been shown that the reaction of the arene−ruthenium(II) complexes[7] [($\eta^6$-arene)$RuCl_2$($PR_3$)] with terminal alkynes and $NaPF_6$ in alcohols directly affords alkoxycarbenes under mild conditions.[8,9] The mechanism of the arene−ruthenium(II) carbene formation involves the formation of [$L_n$Ru($\eta^2$-HC≡CR)] followed by the $\sigma-\pi$ rearrangement, yielding an unstable $\sigma$-vinylidene complex [$L_n$Ru=C=CHR].[10,11] Formation of the alkoxycarbene then proceeds by addition of alcohol to the electrophilic

* Author to whom correspondence should be addressed. E-mail: stepnic@mail.natur.cuni.cz.

⊗ Abstract published in *Advance ACS Abstracts,* October 15, 1997.

(1) Sato, M.; Hayashi, Y.; Kumakura, S.; Shimizu, N.; Katada, M.; Kawata, S. *Organometallics* **1996**, *15*, 721 and references therein.

(2) Beer, P. D.; Kocian, O.; Mortimer, R. J. *J. Chem. Soc., Dalton. Trans.* **1990**, 3283.

(3) (a) Calabrese, J. C.; Cheng, L.-T.; Green, J. C.; Marder, S. R.; Tam, W. *J. Am. Chem. Soc.* **1991**, *113*, 7227 and references therein. (b) Bunting, H. E.; Green, M. L. H.; Marder, S. R.; Thompson, M. E.; Bloor, D.; Kolinsky, P. V.; Jones, R. J. *Polyhedron* **1992**, *11*, 1489 and references therein.

(4) Ghosal, S.; Samoc, M.; Prasad, P. N.; Tufariello, J. J. *J. Phys. Chem.* **1990**, *94*, 2847.

(5) For recent review, see: *Ferrocenes*; Togni, A., Hayashi, T., Eds.; VCH: Weinheim, Germany, 1995.

(6) Pilette, D.; Ouzzine, K.; Le Bozec, H.; Dixneuf, P. H.; Rickard, C. E. F.; Roper, W. R. *Organometallics* **1992**, *11*, 809.

(7) For a review of the reactivity of arene−ruthenium compounds, see: Le Bozec, H.; Touchard, D.; Dixneuf, P. H. *Adv. Organomet. Chem.* **1989**, *29*, 163.

(8) (a) Le Bozec, H.; Ouzzine, K.; Dixneuf, P. H. *Organometallics* **1991**, *10*, 2768. (b) Ouzzine, K.; Le Bozec, H.; Dixneuf, P. H. *J. Organomet. Chem.* **1986**, *317*, C25.

(9) Devanne, D.; Dixneuf, P. H. *J. Organomet. Chem.* **1990**, *390*, 371.

(10) Bullock, R. M. *J. Chem. Soc., Chem. Commun.* **1989**, 165.

(11) Silvestre, J.; Hoffmann, R. *Helv. Chim. Acta* **1985**, *68*, 1461 (theoretical study).

S0276-7333(97)00478-0 CCC: $14.00 

vinylidene $C_\alpha$ carbon. The lower stability of arene−vinylidenes toward nucleophiles in comparison with that of their isoelectronic Cp analogues $[(\eta^5\text{-}C_5H_5)Ru(=C=CHR')(PR_3)_2]PF_6$ is the consequence of the different electron-donating ability of the $[(\eta^6\text{-arene})Ru(PR_3)Cl]^+$ and $[(\eta^5\text{-}C_5H_5)Ru(PR_3)_2]^+$ moieties, as confirmed by the trends in the $Ru^{II}/Ru^{III}$ redox potentials of $[(\eta^6\text{-arene})RuCl_2(PR_3)]$ and $[(\eta^5\text{-}C_5H_5)RuCl(PR_3)_2]$.[9] These studies show that the arene−ruthenium derivatives are much more electron deficient than the analogous Cp complexes. On the other hand, the high reactivity of arene−ruthenium(II) vinylidenes can be utilized for the activation of terminal alkynes. The easily accessible complexes $[(\eta^6\text{-arene})RuCl_2(PR_3)]$ (arene = *p*-cymene or hexamethylbenzene; $PR_3 = PMe_3$ or $PPh_3$) have been used as catalysts for regioselective syntheses of enol esters,[12] $\beta$-oxopropyl esters,[13] and $\beta$-oxoalkyl carbamates,[14] for which analogous ruthenium(II)−cyclopentadienyl derivatives were inactive.

Herein, we report the details of the synthesis and spectral characterization of new ($\eta^6$-hexamethylbenzene)ruthenium(II) methoxycarbenes bearing ferrocenyl unit(s) in the phosphine and/or carbene parts of molecule and also the properties of their parent ($\eta^6$-hexamethylbenzene)ruthenium(II) dichlorophosphine complexes. We also describe the electrochemical behavior of these bimetallic and trimetallic complexes as well as their fragmentation in liquid secondary mass spectra and the crystal structure of $[(\eta^6\text{-}C_6Me_6)Ru(=C(OCH_3)CH_2Fc)\{((\eta^5\text{-}C_5H_4PPh_2)Fe(\eta^5\text{-}C_5H_4COOH))\text{-}P\}(Cl)]PF_6\cdot CH_2Cl_2$ (**4a**·$CH_2Cl_2$).

## Results and Discussion

**Syntheses and Characterization.** The starting ferrocene-containing phosphine complexes $[(\eta^6\text{-}C_6Me_6)RuCl_2(L)]$, where L = $FcPPh_2$ (**3**) and Hdpf (**4**; Hdpf = $(\eta^5\text{-}C_5H_4PPh_2)Fe(\eta^5\text{-}C_5H_4COOH)$), were prepared by the cleavage of the chloro bridges in $[(\eta^6\text{-}C_6Me_6)RuCl_2]_2$ on addition of a stoichiometric amount of the corresponding phosphine. These arene−ruthenium complexes and their $PMe_3$ (**1**) and $PPh_3$ (**2**) analogues were then reacted with terminal alkynes (FcC≡CH (**a**), $Me_3SiC{\equiv}CH$ (**b**), and PhC≡CH (**c**)) in the presence of $NaPF_6$ in MeOH/$CH_2Cl_2$ to give the corresponding methoxycarbenes $[(\eta^6\text{-}C_6Me_6)Ru(=C(OCH_3)CH_2R)Cl(L)]PF_6$ (L = phosphine, R = Fc (**1a**, **2a**, **3a**, **4a**), H (**3b**, **4b**), Ph (**3c**, **4c**)) in good yields (Scheme 1). For the preparation of (methoxy)methylcarbenes **3b** and **4b**, the general procedure was used consisting of methanolysis of Si−C bonds in an intermediate formed by the reaction of (trimethysilyl)acetylene.[15] Although the solid benzyl and (ferrocenyl)methyl carbenes seem to be stable in air at room temperature, their methyl analogues exhibit lower stability, especially in solution. This is in accordance with the predominantly steric stabilization of carbenes. The composition and structure of the products were determined by $^1H$ and $^{31}P\{^1H\}$ NMR, infrared and mass spectra, and elemental analyses. At room temperature, the $^1H$ NMR spectra of **3** and **4** show relatively broad lines of the cyclopentadienyl and phenyl protons. Similarly, phosphorus NMR spectra taken at room temperature exhibit the presence of one broad signal with mutually similar coordination shift values: $\Delta_P(\mathbf{3}) = 38.4$ and $\Delta_P(\mathbf{4}) = 37.8$ ($\Delta_P = \delta_P$(complex) − $\delta_P$(free ligand); $\delta_P(FcPPh_2) = -15.3$, $\delta_P$(Hdpf) = −17.6[16] in $C[^2H]Cl_3$). Respecting the steric requirements of the ferrocenyl phosphines, such broadening of the NMR signals can be attributed to a hindered intramolecular motion, resulting in a dynamic equilibrium of conformers. The temperature-dependent $^{31}P\{^1H\}$ NMR spectra of **3** in $C[^2H]Cl_3$ solution revealed the presence of two isomers in *ca.* 4:1 ratio with chemical shifts $\delta_P$ 21.5 and 27.4 at 223 K. When the sample is warmed, the signals broaden to the coalescence point, which was found to be within 263−273 K, followed by sharpening of the single signal ($\delta_P$ 22.5 at 323 K). The $^1H$ NMR spectra of carbenes **2a**−**4c** also exhibit broad lines (especially these of the Cp and Ph protons), but no conformer equilibria were observed. Because of the presence of the chiral ruthenium center in carbenes **1a**−**4c**, the methylene protons in the proton NMR become diastereotopic and remarkably anisochronic (the separation of both signals of the AB system $\Delta\delta_{AB}$ is up to 2.07 ppm for **2a**). This relatively large separation could be tentatively explained by the presence of strongly anisotropically shielding phenyl and ferrocenyl[17] groups in the phosphine part of the molecules (compare with $\Delta\delta_{AB}$ 0.65 for **1a**). In all cases, selective decoupling was used to identify the low-field component of the AB system, which often coincides with the broad and strong signals of the Cp and methoxy protons. For **3a** and **4a**, anisochronicity of the α-protons of carbene cyclopentadienyl was observed while the $\beta$-protons remain unresolved. Except for **1a**, $^{13}C$ NMR spectra of the carbenes could not be obtained in sufficient quality due to the broadening caused by intramolecular motion which is slow in the NMR scale. Signals arising from

**Scheme 1**

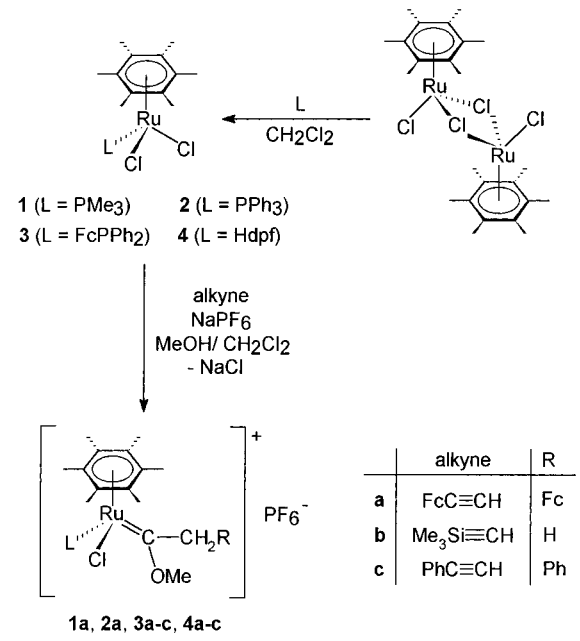


**1a**, **2a**, **3a-c**, **4a-c**

Fc = ferrocenyl, Hdpf = $(\eta^5\text{-}C_5H_4PPh_2)Fe(\eta^5\text{-}C_5H_4COOH)$

(12) Ruppin, C.; Dixneuf, P. H. *Tetrahedron Lett.* **1986**, *27*, 6323.
(13) Devanne, D.; Dixneuf, P. H. *J. Org. Chem.* **1988**, *53*, 925.
(14) Bruneau, C.; Dixneuf, P. H. *Tetrahedron Lett.* **1987**, *28*, 2005.
(15) Parlier, A.; Rudler, H. *J. Chem. Soc., Chem. Commun.* **1986**, 514.
(16) Podlaha, J.; Štěpnička, P.; Ludvík, J.; Císařová, I. *Organometallics* **1996**, *15*, 543.
(17) Turbitt, T. D.; Watts, W. E. *Tetrahedron* **1972**, *28*, 1227.

**Table 1. Crystallographic Data for 4a·$CH_2Cl_2$**

| | |
|---|---|
| formula | $C_{49}H_{53}F_6O_3P_2Cl_3Fe_2Ru$ |
| $M$ | 1184.97 |
| cryst syst; space group | triclinic; $P\bar{1}$ (No. 2) |
| $a$ (Å); α (deg) | 12.072(1); 104.11(1) |
| $b$ (Å); $\beta$ (deg) | 14.470(2); 99.663(8) |
| $c$ (Å); $\gamma$ (deg) | 14.999(2); 93.773(9) |
| $V$ (Å$^3$); $Z$ | 2489.3(5); 2 |
| $D_c$ (g·mL$^{-1}$) | 1.581 |
| $F$(000) | 1204 |
| cryst size (mm$^3$) | 0.05 × 0.2 × 0.3 |
| cryst description | orange-red plate |
| $\mu$ (mm$^{-1}$) | 1.16 |
| 2$\theta$ range (deg) | 2.8−46.0 |
| $hkl$ | $+h, \pm k, \pm l$ |
| no. of diffractions collected; $R(\sigma)$[a] | 6941; 15.0 |
| no. of unique diffractions | 6910 |
| no. of obsd diffractions; $F_o \geq 4\sigma(F_o)$ | 3725 |
| standard diffractions | 3 monitored every 1 h |
| variation in standards (%) | 2.9 |
| weighting scheme: $w_1$, $w_2$[b] | 0.0895, 8.6931 |
| no. of params | 584 |
| $R_{all}(F)$, $R_{obs}(F)$[a] (%) | 17.5, 6.9 |
| $wR_{all}(F^2)$, $wR_{obs}(F^2)$[a] (%) | 20.8, 16.3 |
| $GOF_{all}$[a] | 1.03 |
| $(\Delta/\sigma)_{max}$ | 0.000 |
| $\Delta\rho$ (e·Å$^{-3}$) | 1.11, −0.82 |

[a] $R(F) = \sum(||F_o| - |F_c||)/\sum|F_o|$, $wR(F^2) = \sum[(w(F_o^2 - F_c^2)^2)/(w(F_o^2)^2]^{1/2}$, $GOF = [\sum(w(F_o^2 - F_c^2)^2)/(N_{diffrs} - N_{params})]^{1/2}$, $R(\sigma) = \sum\sigma(F_o^2)/\sum F_o^2$. [b] Weighting scheme: $w = [\sigma^2(F_o^2) + w_1P^2 + w_2P]^{-1}$; $P = [\max(F_o^2) + 2F_c^2]/3$.

the Ru=C(OCH$_3$)CH$_2$Fc moiety in the $^{13}C\{^1H\}$ NMR spectrum of **1a** were found within the expected region:[8] Ru=*C* $\delta_C$ 320.7 (d, $^2J_{PC}$ = 22 Hz), O*C*H$_3$ $\delta_C$ 67.6, and *C*H$_2$ $\delta_C$ 50.2, as these clearly indicate the presence of carbene. The assignment was supported by DEPT-135. The decrease of electron density on changing the neutral dichloro complex to the cationic carbene also results in a significant downfield shift of the coordinated phosphine signal in the $^{31}P\{^1H\}$ NMR spectra. The coordination shift is practically independent of the nature of the substituent R linked to the carbene part, as demonstrated by the similarity of its value for **3a**−**c** $\Delta_P \approx$ 48 and **4a**−**c** $\Delta_P \approx$ 50 (*cf.* $\Delta_P$(**2a**) = 39.8, $\delta_P(PPh_3) = -4.1$ was obtained under the same conditions). These spectral features are in agreement with the observed electrochemical response of carbenes **1a**−**4c**.

**Crystal Structure.** A single crystal X-ray diffraction study of **4a**·$CH_2Cl_2$ was carried out to confirm the solid-state structure of carbenes. The crystallographic data are given in Table 1 and the Experimental Section. A listing of selected bond lengths and angles is given in Table 2. As the hexafluorophosphate counterion and solvating dichloromethane do not display any unexceptional features, the organometallic cation is the only interesting part of the present structure. The cation of **4a** is chiral due to the presence of four different substituents in a three-legged piano-stool structure; the ($R_{Ru}$)-[($\eta^6$-$C_6Me_6$)Ru(=C(OCH$_3$)CH$_2$Fc){(($\eta^5$-$C_5H_4$-PPh$_2$)Fe($\eta^5$-$C_5H_4$COOH))-*P*}(Cl)]$^+$ enantiomer was arbitrarily chosen in the refinement (Figure 1, PLATON92[18]). In the racemic crystal, both enantiomeric cations are joined through double centrosymmetric hydrogen bonds: O(2)···O(1)$^i$ 2.58(2) Å, $i = -x, -y, 1 - z$ which are, however, distorted by the presence of the neighboring dichloromethane molecule: O(2)···Cl(9A)$^i$ 3.44(2) Å, O(1)···Cl(9A) 4.07(2) Å. There are no further significant intermolecular contacts except those at the van der Waals level. In the molecular structure of the cation, the $\eta^6$-hexamethylbenzene ring and the monodentate ligands are mutually staggered and the $\eta^6$-arene ring is bent about the C(02)−C(05) axis; the dihedral angle of the half planes defined by C(02), C(03), C(04), C(05) and C(05), C(06), C(01), C(02), respectively, is to 8.5(8)°. A similar feature was observed for [($\eta^6$-$C_6H_6$)-RuCl$_2$(PMePh$_2$)] and [($\eta^6$-*p*-MeC$_6$H$_4$CHMe$_2$)RuCl$_2$-(PMePh$_2$)].[19] The length of the Ru−Cl bond is close to the mean value found for Ru complexes (2.42(5) Å, 115 structures[20]) and the Ru−P bond length similar to that of Ru−PPh$_2$Me (2.40(6) Å, 4 structures; *cf.* Ru−PPh$_3$ 2.37(4) Å, 59 structures; Ru−PMe$_3$ 2.31(5) Å, 65 structures). The carbene Ru=C bond (1.94(1) Å) is slightly

**Table 2. Selected Bond Lengths (Å) and Angles (deg) for 4a·$CH_2Cl_2$**

| | | | |
|---|---|---|---|
| Ru−C($C_6Me_6$, av) | 2.31(6) | C−C−C($C_6Me_6$, av) | 119(2) |
| $C_{ar}$−$C_{ar}$(av) | 1.41(2) | | |
| $C_{ar}$−$CH_3$(av) | 1.53(1) | | |
| Ru−Cl | 2.390(3) | Cl−Ru−C(61) | 93.2(4) |
| | | Cl−Ru−P(1) | 85.5(1) |
| | | P(1)−Ru−C(61) | 87.0(3) |
| Ru−C(61) | 1.94(1) | O(3)−C(61)−C(63) | 117(1) |
| O(3)−C(61) | 1.30(1) | C(61)−O(3)−C(62) | 127(1) |
| O(3)−C(62) | 1.46(2) | C(61)−C(63)−C(71) | 114.4(9) |
| C(61)−C(63) | 1.52(2) | O(3)−C(61)−Ru | 116.6(8) |
| C(63)−C(71) | 1.53(2) | C(63)−C(61)−Ru | 126.3(9) |
| C−C(Fc, av) | 1.38(4) | C(75)−C(71)−C(63) | 126(1) |
| Fe−C(av) | 2.01(3) | C(72)−C(71)−C(63) | 127(1) |
| | | C−C−C(Fc, av) | 108(3) |
| Ru−P(1) | 2.343(3) | C(21)−P(1)−Ru | 112.5(4) |
| P(1)−C(21) | 1.83(1) | C(41)−P(1)−Ru | 117.5(4) |
| P(1)−C(41) | 1.82(1) | C(51)−P(1)−Ru | 115.3(3) |
| P(1)−C(51) | 1.83(1) | C(21)−P(1)−C(41) | 103.1(5) |
| C(31)−C(36) | 1.46(2) | C(21)−P(1)−C(51) | 105.9(5) |
| C(36)−O(1) | 1.24(2) | C(41)−P(1)−C(51) | 101.0(5) |
| C(36)−O(2) | 1.29(2) | O(1)−C(36)−O(2) | 123(1) |
| C−C(Fc, av) | 1.41(2) | O(1)−C(36)−C(31) | 119(1) |
| Fe−C(av) | 2.04(2) | O(2)−C(36)−C(31) | 118(1) |
| C−C(Ph, av) | 1.38(2) | C(32)−C(31)−C(36) | 128(1) |
| | | C(35)−C(31)−C(36) | 126(1) |
| | | C−C−C(Fc, av) | 108.0(9) |
| | | C−C−C(Ph, av) | 120(1) |
| P(2)−F(av) | 1.47(6) | F−P(2)−$F_{cis}$(av) | 90(4) |
| C(9A)−Cl(9A) | 1.65(4) | Cl(9A)−C(9A)−Cl(9B) | 108(2) |
| C(9A)−Cl(9B) | 1.79(4) | | |

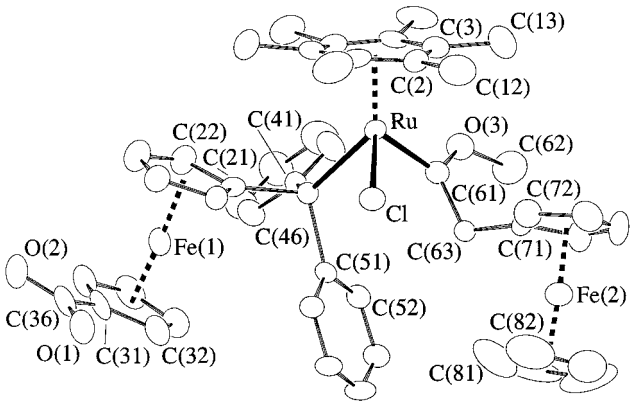


**Figure 1.** PLATON plot of the molecule ($R_{Ru}$)−**4a**·$CH_2Cl_2$ at the 30% probability level. The $PF_6^-$ anion, the solvating dichloromethane molecule, and all hydrogens are omitted.

(18) Spek, A. L. *Acta Crystallogr.* **1990**, *A46*, C34.

(19) Bennett, M. A.; Robertson, G. B.; Smith, A. K. *J. Organomet. Chem.* **1972**, *43*, C41.

(20) Orpen, A. G.; Brammer, L.; Allen, F. H.; Kennard, O.; Watson, D. G.; Taylor, R. *J. Chem. Soc., Dalton Trans.* **1989**, S1.

**Table 3. Redox Potentials of Ruthenium Complexes in $CH_2Cl_2$[a]**

| compound | $E^{Fc}$ [V] | |
|---|---|---|
| | $Fc/Fc^+$ | $Ru^{II}/Ru^{III}$ |
| **1** | | 0.39 |
| **2** | | 0.48 |
| **3** | 0.03(P)[b] | 0.66 |
| **4** | 0.28(P) | 0.68 |
| **1a** | 0.08(C) | 0.90 |
| **2a** | 0.09(C) | 1.12 |
| **3a** | 0.05(C), 0.27(P) | 1.08 |
| **3b** | 0.22(P) | 1.07 |
| **3c** | 0.27(P) | 1.15 |
| **4a** | 0.06(C), 0.52(P) | 1.12 |
| **4b** | 0.45(P) | 1.09 |
| **4c** | 0.50(P) | 1.16 |

[a] All observed redox processes exhibit a peak separation $\Delta E_p$ in the range of 75−95 mV and $(i_{pa}/i_{pc})$ values of unity. Potentials are given relative to ferrocene/ferrocenium, $E^{Fc} = {}^1/_2(E_{pa} + E_{pc})$. Derivative cyclic voltammetry was used for $E_p$ and $i_p$ determination. For further experimental details, see Experimental Section. [b] P and C denotes the ferrocenyl group in the phosphine and carbene parts of molecule, respectively.



shortened in comparison with that of the vinylidene[21] complex $[(\eta^6\text{-}C_6Me_6)Ru(=C(OCH_3)CH=CPh_2)(Me_3P)Cl]PF_6$ (1.98 Å) because of the absence of conjugation. The carbene moiety is planar [$\tau$(C(62)−O(3)−C(61)−C(63)) = −1(2)°] without any significant difference from the average bond lengths reported for carbenes of the $[L_nRu=C(OC')C'']$ type (C−C″ 1.50(3) Å, C−O 1.32(2) Å, O−C′ 1.47(2) Å; 18 structures[20]). The carbene ferrocenyl does not show any deformation (the dihedral angle of the least-squares Cp planes 4(2)°) apart from a slight dynamic disorder of the unsubstituted Cp ring along the $D_5$ axis. The general geometry of carboxyphosphine ferrocenyl remains practically unaffected by coordination (the dihedral angle of Cp ring planes 5.6(9)°, C−P−C angles similar to those of noncoordinated Hdpf[16]). The only significant difference is the relative conformation of the carboxy and diphenylphosphino groups, which are *anti*-eclipsed with the torsion angle $\tau$(P(1)−CE(1)−CE(2)−C(36)) −148.1(5)°; in contrast, noncoordinated Hdpf occupies a halfway *anti*-conformation with the $\tau$ value of *ca.* −162°. As the rotational barrier along the $D_5$ axis is known to be low, such changes are invoked most likely by crystal packing effects, the H bond formation being one of the most significant.

**Electrochemistry**. For all compounds, the electrochemical study revealed that all observed redox processes are one-electron and reversible processes at the scan rate of 1 $V\cdot s^{-1}$, as indicated by the $(i_{pa}/i_{pc})$ ratios of unity and the $\Delta E_p$ peak separations in the range of 75−95 mV. The redox potentials $E^{Fc}$ given relative to ferrocene/ferrocenium[22] are summarized in Table 3. The cyclic voltammograms of the starting chloro complexes **1** and **2** display only one wave from the $Ru^{II}/Ru^{III}$ redox couple. The easier oxidation of **1** in comparison to **2** is in accordance with the higher electron-donating ability of the $PMe_3$ ligand. The presence of ferrocenyl-bearing phosphines in complexes **3** and **4**, reflected by the appearance of the additional wave of the $Fc/Fc^+$ couple, strongly modifies the properties of both electrochemically active parts of the complex. First, the presence of ferrocenyl phosphine causes a relative increase of the $Ru^{II}/Ru^{III}$ potential and, simultaneously, the decrease of the ferrocene/ferrocenium potential. For illustration, $E^{Fc}(FcPPh_2) = 0.11$ V with $\Delta E_p = 80$ mV and $(i_{pa}/i_{pc}) \approx 0.4$ at the same conditions; for Hdpf, only the anodic peak potential could be detected at the scan rate of 1 $V\cdot s^{-1}$, $E_{pa}^{Fc} = 0.39$ V. Second, there is an apparent contradiction with the expected trend, *i.e.*, the decrease of the electron density in the ligand moiety on dative bond formation, which causes an increase of the potential of the ligand-centered redox process. This common trend could be illustrated by the potentials of the following (diphenylphosphino)ferrocene complexes: $[(FcPPh_2)M(CO)_5]$, M = Mo $E^{Fc} = 0.27$ V; W $E^{Fc} = 0.29$ V; while for noncoordinated $FcPPh_2$, $E^{Fc} = 0.11$ V.[23] Such an unexpected electrochemical response for **3** and **4** could be attributed to a significant contribution of the Ru ← P $\pi$-back-donation, resulting in a decrease of the electron-withdrawing properties of the diphenylphosphino group and, in this way, relative increase of the electron density within the ferrocenyl moiety. At a higher potential, the ferrocenium formed in the first oxidative step undergoes a successive ruthenium-centered oxidation. However, the presence of the strongly electron-withdrawing ferrocenium makes this step more difficult in comparison with simple phosphines containing complexes **1** and **2**, as indicated by the shift to higher potentials. Thus, by modification of the phosphine substituent, the $Ru^{II}/Ru^{III}$ potential shifted to a higher value although, taking into account the electron-donating ability of the ferrocenyl group, the potential could be *a priori* expected between those of **1** and **2**. The coordination also stabilizes both ferrocenyl phosphines toward subsequent reactions[16] of the ferricinum species yielding phosphine oxides. While free ferrocenyl phosphines exhibit quasi-reversible waves reflecting the subsequent decomposition of the generated ferrocenium, the values of $(i_{pa}/i_{pc}) \approx 1$ observed for the phosphine-centered redox step indicate reversible ferrocene−ferrocenium processes in the case of **3**, **4**, **3a**−**c**, and **4a**−**c**. An analogous stabilization has been reported for (diphenylphosphino)ferrocene complexes of molybdenum and tungsten (*vide infra*). Similarly, when not stabilized by the formation of stable complexes such as $[M(dppf\text{-}P,P')Cl_2]$, M = Pd, Pt,[24] free 1,1′-bis(diphenylphosphino)ferrocene (dppf) is oxidized to ferrocenium and immediately converted to protonated and higher oxidized species.[25]

The change of the electrochemical response of the carbene complexes in comparison to the neutral parent chloro complexes is consistent with generation of cationic species (Figure 2). The electron density decrease makes oxidation of $Ru^{II}$ markedly more difficult, as documented by the positive shift of about 0.5 V for the ruthenium-centered oxidation. This change also affects the phosphine part of the molecule, as manifested by the anodic shift of approximately +0.2 V for the $Fc/Fc^+$

(21) Structure VOYDOC in Cambridge Crystallographic Data Centre; for reference see: Allen, F. H.; Kennard, O. *Chem. Design Automat. News* **1993**, *8*, 1, 31−37.

(22) $E^{SCE} = E^{Fc} + E^{SCE}(FcH/FcH^+)$; $E^{SCE}(FcH/FcH^+) = +0.46$ V in $CH_2Cl_2$, 0.1 M $BuN_4PF_6$. For ref, see: Connelly, N. G.; Geiger, W. E. *Chem. Rev.* **1996**, *96*, 877.

(23) Kotz, J. C.; Nivert, C. L.; Lieber, J. M.; Reed, R. C. *J. Organomet. Chem.* **1975**, *91*, 87.

(24) Corain, B.; Longato, B.; Favero, G.; Ajó, D.; Pilloni, G.; Russo, U.; Kreissl, F. R. *Inorg. Chim. Acta* **1989**, *157*, 259.

(25) Pilloni, G.; Longato, B.; Corain, B. *J. Organomet. Chem.* **1991**, *420*, 57.

**Table 4. Mass Spectrometric Characteristics of Carbenes [($\eta^6$-HMB)Ru(=C(OCH$_3$)CH$_2$R)(L)Cl]PF$_6$[a]**

| compound (L/R) | 1a (PMe$_3$/Fc) | 2a (PPh$_3$/Fc) | 3a (FcPPh$_2$/Fc) | 3b (FcPPh$_2$/H) | 3c (FcPPh$_2$/Ph) | 4a (Hdpf/Fc) | 4b (Hdpf/H) | 4c (Hdpf/Ph) |
|---|---|---|---|---|---|---|---|---|
| [cation]$^+$ | 617(100) | 803(17) | 911(100) | 727(11) | 803(100) | 955(79) | 771(7) | 847(94) |
| [cation − HCl]$^+$ | 581(2) | weak | 875(2) | weak | 767(3) | weak | | 811(3) |
| [cation − HMB − HCl]$^+$ | 419(11) | 605(8) | 713(22) | | 605(10) | 757(21) | | 649(42) |
| [cation − C(OCH$_3$)CH$_2$R]$^+$ | 375(40) | 561(9) | 669(10) | 669(12) | 669(3) | 713(6) | 713(26) | 713(3) |
| [cation − C(OCH$_3$)CH$_2$R − HCl]$^+$ | <350 | 525(13) | 633(6) | 633(3) | 633(3) | 677(40) | 677(46) | 677(16) |
| [cation − L]$^+$ | 541(3) | 541(9) | 541(42) | 357(14) | 433(48) | 541(100) | 357(12) | 433(100) |
| [cation − L − HCl]$^+$ | | 505(6) | 505(10) | weak | 397(18) | 505(29) | 321(22) | 397(51) |
| L$^+$ | <350 | <350 | 370(97) | 370(100) | 370(81) | 414(29) | 414(100) | 414(35) |
| [LCH$_2$R]$^+$ | <350 | 461(100) | 569(29) | | | | | |
| [cation − CpFe − HMB − Cl]$^+$ | <350 | 485(16) | 593(45) | weak | 485(19) | 637(25) | | |
| [cation − C$_6$H$_5$O$_2$Fe − HMB − Cl]$^+$ | | | | | | 593(14) | | 485(24) |
| [cation − CpFe − C(OCH$_3$)CH$_2$R − HCl]$^+$ | <350 | <350 | 513(18) | 513(12) | 513(8) | | | |
| [cation − C$_6$H$_5$O$_2$Fe − C(OCH$_3$)CH$_2$R − HCl]$^+$ | | | | | | 513(21) | 513(54) | 513(14) |
| other | | | | | 641(8)[b] | 887(22)[c] | | 779(8)[c] |

[a] LSIMS data obtained in a 3-nitrobenzyl alcohol matrix. The signals with $m/z$ > 350 only are listed as $m/z$(relative intensity). HMB = hexamethylbenzene, L = phosphine. [b] [cation − HMB]$^+$. [c] [cation − 68]$^+$, possible elimination of HCl and MeOH.

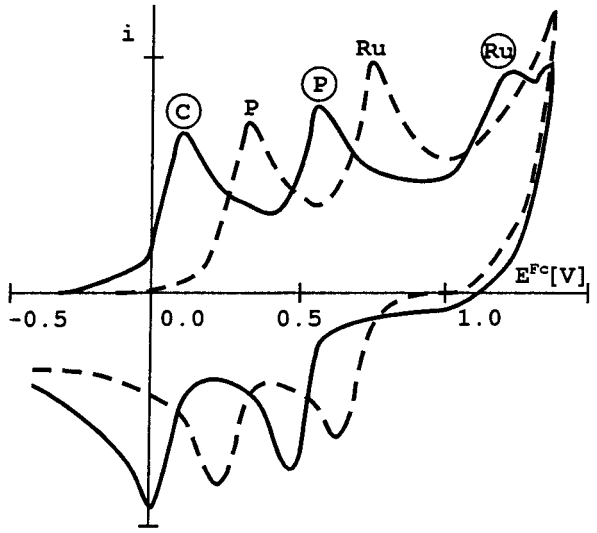


**Figure 2.** Cyclic voltammetric response of **4** (broken line) and **4a** (full line). C, P, and Ru denote carbene ferrocenyl, phosphine ferrocenyl, and ruthenium-centered redox processes, respectively (circled for **4a**).

potential. This is most likely caused by an electron-density transfer from phosphine to ruthenium, which cannot be compensated by back-donation from the now electron-deficient metal. Similar trends in the Fc/Fc$^+$ potential were observed in the case of the (diphenylphosphino)ferrocene carbonyl complexes of molybdenum and tungsten mentioned above, in which the contribution of the back-donation from the metal to phosphorus could be expected to be weak due to the presence of five good $\pi$-accepting carbonyl ligands. Moreover, replacement of the electron-withdrawing ethynyl group by an electron-donating alkyl returns the carbene Fc/Fc$^+$ potential in **1a**, **2a**, **3a**, and **4a** to values close to those of unsubstituted ferrocene (*cf.* FcC≡CH $E^{Fc}$ = 0.16 V, $\Delta E_p$ = 75 mV, $i_{pa}/i_{pc}$ = 1.0 under the same conditions). These potentials are practically unaffected by changes on the metal center. Likewise, the Ru$^{II}$/Ru$^{III}$ potentials exhibit only a small variation on changing the substituent in the carbene part, as indicated by the trends in **3a**−**c** and **4a**−**c**. These facts clearly imply an interruption of electronic communication, except for simple inductive effects, between L$_n$Ru=C and the carbene substituent R (Ru=C(OCH$_3$)CH$_2$R) on introduction of a CH$_2$ spacer.

**Mass Spectrometry.** The positive-mode secondary ion mass spectra of the complexed salts **1a**, **2a**, **3a**−**c**, and **4a**−**c** exclusively exhibit the signals of the free organometallic cations and their fragment ions, most likely owing to the dissociation of the ionic carbenes dissolved in the matrix. Nevertheless, the presence of the hexafluorophosphate counterion is obvious from the presence of weak signals due to the formation of clusters [cation$_2$, PF$_6^-$]$^+$. In general, the cations undergo fragmentation by splitting of ruthenium-bonded ligands, *i.e.*, the carbene part, hexamethylbenzene, or phosphine, together or without the elimination of HCl (Table 4). While fragment ions corresponding to the loss of the phosphine or carbene part with or without concurrent elimination of HCl are easily observable; the peaks corresponding to the loss of C$_6$Me$_6$ or HCl are weak or not observed at all. On the other hand, the simultaneous loss of C$_6$Me$_6$ and HCl results in peaks of considerable intensity, with the exception of methyl carbenes **3b** and **4b**. All spectra also display the presence of positively charged free phosphines. In the case of **2a** and **3a**, further peaks appear in the spectra which correspond to phosphonium ions resulting by the migration of the carbene substituent (RCH$_2$ in [L$_n$Ru(=C(OCH$_3$)CH$_2$R)]$^+$) to phosphine phosphorus. It is worth noting that the presence of the ferrocene skeleton in all cases leads to the occurrence of less common ionic species in the spectra. Their formation involves elimination of cyclopentadienyl−iron ([C$_5$H$_5$Fe]$^+$) or carboxycyclopentadienyl−iron ([C$_6$H$_5$O$_2$Fe]$^+$) fragments arising from phosphine or carbene ferrocenyls.

The mass spectra of dichloro complexes **3** and **4** exhibit positively charged molecular ions and fragments [M − $n$Cl]$^+$ ($n$ = 1, 2). Although the loss of the phosphine molecule has not been observed here, the charged phosphines, [FcPPh$_2$]$^+$ and [Hdpf]$^+$, appear as the most intense peaks in the spectra (for low-resolution mass spectral data, see Experimental Section). A further notable feature similar to that in the carbenes is the presence of the ionic species $m/z$ 513 due to the simultaneous loss of two chlorine atoms and [C$_5$H$_5$Fe]$^+$ and [C$_6$H$_5$O$_2$Fe]$^+$ for **3** and **4**.

## Concluding Remarks

We described the syntheses of several new ferrocenyl-substituted ruthenium(II) carbenes. These compounds were studied with respect to their structure and electronic properties by multinuclear NMR spectroscopy and

electrochemistry in solution and by single-crystal X-ray diffraction in the solid state. From the electrochemical behavior of the ferrocenyl phosphines bearing ($\eta^6$-hexamethylbenzene)chlororuthenium(II) methoxycarbenes and their parent ($\eta^6$-hexamethylbenzene)dichlororuthenium(II) complexes, it follows that there is no electronic communication between the $L_nRu{=}C$ moiety and the carbene substituent, excluding inductive effects. On the other hand, the presence of the oxidized phosphine ligand (formation of *P*-coordinated ferrocenium precedes the $Ru^{II} \rightarrow Ru^{III}$ oxidation) results in a significant electron density lowering at the central atom. Such a modification of the electronic properties of the metal center in catalytically important organometallic compounds by changing the oxidation state of ligand(s) might be used for fine "tuning" their catalytic properties.

## Experimental Section

**General Considerations.** All experiments were carried out in an atmosphere of argon or nitrogen using Schlenk techniques. The solvents were dried and deoxygenated by standard procedures. $^1$H (200.13 MHz), $^{31}$P{$^1$H} (81.02 MHz), and $^{13}$C{$^1$H} (50.33 MHz) NMR spectra were recorded on a Bruker DPX200 spectrometer at 296 K with external tetramethylsilane ($^1$H, $^{13}$C) and external 85% aqueous $H_3PO_4$ ($^{31}$P) as the standards. Liquid secondary-ion mass spectral (LSIMS) data were obtained on a VG ZabSpec spectrometer (CRMPO center, University of Rennes) operating in a positive-ion mode using CsI as the primary ion source and 3-nitrobenzyl alcohol as the matrix. For high-resolution measurements (HRMS), poly(ethylene glycol) was used as the mass scale calibrant. IR spectra were recorded on a Nicolet 205 spectrometer in KBr pellets. Cyclic voltammograms were measured in an argon atmosphere with $1 \times 10^{-3}$ M dichloromethane solutions containing 0.1 M $Bu_4NPF_6$ as the supporting electrolyte at the scan rate of 1 V·s$^{-1}$. The measurements were carried out using a potentiostat (model 263, EG&G Princeton Applied Research) connected to an oscilloscope (Nicolet 310), a wave form generator (Hewlett-Packard 33120A), and a selective amplifier (model 189, EG&G Princeton Applied Research) with platinum discs of 0.4 mm diameter as the working and auxiliary electrodes and a saturated calomel electrode as the reference. The potentials are given relative to ferrocene/ferrocenium; a calibration cyclic voltammogram of ferrocene was registered before each measurement. Elementary analyses were performed by the CNRS Service Central d'Analyses (Vernaison, France). $[(\eta^6\text{-}C_6Me_6)Ru(\mu\text{-}Cl)Cl]_2$,[26] $[(\eta^6\text{-}C_6Me_6)Ru(L)Cl_2]$[27] (L = $PMe_3$ (**1**), $PPh_3$ (**2**)), FcC≡CH,[28] $FcPPh_2$,[29] and Hdpf[16] were prepared according to the published procedures.

**Preparation of ($\eta^6$-Hexamethylbenzene)$RuCl_2$(phosphine) Complexes, $[(\eta^6\text{-}C_6Me_6)Ru(FcPPh_2)Cl_2]$ (3).** To a stirred solution of $[(\eta^6\text{-}C_6Me_6)Ru(\mu\text{-}Cl)Cl]_2$ (0.667 g, 1.00 mmol) in dichloromethane (50 mL), $FcPPh_2$ (0.750 g, 2.03 mmol) was added in one portion and the mixture was stirred for 90 min at room temperature. After evaporation under reduced pressure, the product was washed with diethyl ether (25 mL) and pentane (2 × 25 mL) and dried *in vacuo* to give **3** (1.283 g, 91%) as an orange-red solid. $^1$H NMR (C[$^2$H]$Cl_3$): $\delta$ 1.75 (d, $^4J_{PH}$ = 0.5 Hz, 18 H, $C_6Me_6$), 3.78 (s, 5 H, $C_5H_5$), 4.42 (br s, 2 H, $C_5H_4$), 4.56 (br s, 2 H, $C_5H_4$), 7.34−7.46 (m, 6 H, $PPh_2$), 7.85−8.01 (m, 4 H, $PPh_2$). $^{31}$P{$^1$H} NMR (C[$^2$H]$Cl_3$): $\delta$ 22.3 (br s). IR (cm$^{-1}$): $\nu$(CH) 3049 (w), 2908 (w); $\delta_s(CH_3)$ 1383 (m); Fc 1096 (m), 1002 (m); $PPh_2$ 470 (s, composed). Anal. Calcd for $C_{34}H_{37}PCl_2FeRu$: C, 57.97; H, 5.29; P, 4.40. Found: C, 58.07; H, 5.41 P, 4.20. HR LSIMS: *m*/*z* $[C_{34}H_{37}PCl_2FeRu]^+$ ($M^+$) calcd 704.0409, found 704.039; $[C_{34}H_{37}PClFeRu]^+$ ([M − Cl]$^+$), calcd 669.0723, found 669.072. LSIMS: *m*/*z* (relative intensity) 704 (6, $M^+$), 669 (25, [M − Cl]$^+$), 633 (3, [M − 2Cl]$^+$), 513 (15, [M − 2Cl − $C_5H_5Fe$]$^+$), 370 (100, $[FcPPh_2]^+$).

**[($\eta^6$-$C_6Me_6$)Ru(Hdpf-*P*)$Cl_2$] (4).** Starting from $[(\eta^6\text{-}C_6Me_6)Ru(\mu\text{-}Cl)Cl]_2$ (0.667 g, 1.00 mmol) and Hdpf (0.829 g, 2.00 mmol), the same procedure as for **3** yielded **4** (1.470 g, 98%) as an orange-red solid. $^1$H NMR (C[$^2$H]$Cl_3$): $\delta$ 1.75 (s, 18 H, $C_6Me_6$), 3.74 (s, 2 H, $C_5H_4$), 4.50 (s, 4 H, $C_5H_4$), 4.60 (s, 2 H, $C_5H_4$), 7.33−7.52 (br s, 6 H, $PPh_2$), 7.78−7.98 (br s, 4 H, $PPh_2$). $^{31}$P{$^1$H} NMR (C[$^2$H]$Cl_3$): $\delta$ 20.2 (br s). IR (cm$^{-1}$): $\nu$(CH) 3050 (w), 2982 (w); $\nu$(C=O) 1712 (m), 1686 (s); $\delta_s(CH_3)$ 1385 (m); Fc 1096 (m), 1035 (m); $PPh_2$ 490 (s, composed). Anal. Calcd for $C_{35}H_{37}O_2PCl_2FeRu$: C, 56.17; H, 4.98; P, 4.14. Found: C, 55.89; H, 4.90; P, 4.01. HR LSIMS: *m*/*z* $[C_{35}H_{37}O_2PCl_2FeRu]^+$ ($M^+$) calcd 748.0308, found 748.032; $[C_{35}H_{37}O_2PClFeRu]^+$ ([M − Cl]$^+$), calcd 713.0621, found 713.060. LSIMS: *m*/*z* (relative intensity) 748 (6, $M^+$), 713 (35, [M − Cl]$^+$), 677 (66, [M − 2Cl]$^+$), 513 (15, [M − 2Cl − $C_6H_5O_2Fe$]$^+$), 414 (100, [Hdpf]$^+$).

**General Procedure for Preparation of Carbenes.** The starting ruthenium(II) complex $[(\eta^6\text{-}C_6Me_6)RuCl_2(phosphine)]$ (0.5 mmol) and $NaPF_6$ (0.5 mmol or slight excess) were dissolved in methanol (25 mL) and dichloromethane (25 mL; except for **1a**), and an excess of alkyne was added. The mixture was stirred at room temperature for 90 min (the progress of reaction causes color lightening), and the resulting solution was evaporated under reduced pressure. After the solid was washed with diethyl ether (3 × 20 mL; removal of unreacted alkyne) and dried *in vacuo*, the solid residue was dissolved in dichloromethane (10 mL) and the solution filtered *via cannula* to remove NaCl. After addition of pentane (40 mL) to the filtrate, the biphasic mixture was left to crystallize on diffusion at −20 °C for several days. Decantation of the solvent mixture followed by washing with pentane (20 mL) and drying *in vacuo* afforded solid carbenes.

**[($\eta^6$-$C_6Me_6$)Ru(=C($OCH_3$)$CH_2$Fc)($PMe_3$)(Cl)] (1a).** **1** (206 mg, 0.50 mmol), $NaPF_6$ (86 mg, 0.51 mmol) and FcC≡CH (316 mg, 1.50 mmol) gave **1a** (310 mg, 81%) as ruby-red crystals. The reaction was carried out in methanol (25 mL) without addition of dichloromethane. $^1$H NMR (C[$^2$H]$Cl_3$): $\delta$ 1.47 (d, $^2J_{PH}$ = 10.6 Hz, 9 H, $PMe_3$), 2.04 (s, 18 H, $C_6Me_6$), 4.20 (br m, 2 H, $C_5H_4$), 4.22 (d, $^2J_{HH}$ = 12.6 Hz, 1 H, AB $CH_2$), 4.23 (s, 5 H, $C_5H_5$), 4.31 (s, 2 H, $C_5H_4$), 4.69 (s, 3 H, O*Me*), 4.87 (d, $^2J_{HH}$ = 12.6 Hz, 1 H, AB $CH_2$). $^{31}$P{$^1$H} NMR (C[$^2$H]$Cl_3$): $\delta$ −143.1 (sept, $^1J_{PF}$ = 712 Hz, $PF_6^-$), 9.1 (s, $PMe_3$). $^{13}$C{$^1$H} NMR (C[$^2$H]$Cl_3$): $\delta$ 16.2 (d, $^1J_{PC}$ = 34 Hz, $PMe_3$), 16.8 (s, $C_6Me_6$), 50.2 (s, $CH_2$), 67.6 (s, O*Me*), 68.9 (d, $^2J_{PC}$ = 31 Hz, $C_5H_4$, $C_\alpha$), 70.1 (s, $C_5H_5$), 72.2 (s, $C_5H_4$, $C_\beta$), 78.5 (d, $^1J_{PC}$ = 86 Hz, $C_5H_4$, $C_{ipso}$), 107.6 (d, $^2J_{PC}$ = 2 Hz, $C_6Me_6$), 320.7 (d, $^2J_{PC}$ = 22 Hz, Ru=C). IR (cm$^{-1}$): $\nu$(CH) 3094 (w), 2920 (w); $\delta_s(CH_3)$ 1385 (m); $\nu$(C−O) 1275 (s); Fc 1052 (m), 954 (m); $PF_6^-$ 839 (s); $PPh_2$ 482 (s). Anal. Calcd for $C_{28}H_{41}OF_6P_2ClFeRu$: C, 44.14; H, 5.42; P, 8.13. Found: C, 44.64; H, 5.40; P, 7.87. HR LSIMS: *m*/*z* $[C_{28}H_{41}OPClFeRu]^+$ ([M − $PF_6$]$^+$), calcd 617.0983, found 617.095.

**[($\eta^6$-$C_6Me_6$)Ru(=C($OCH_3$)$CH_2$Fc)($PPh_3$)(Cl)] (2a).** **2** (299 mg, 0.50 mmol), $NaPF_6$ (86 mg, 0.51 mmol) and FcC≡CH (210 mg, 1.00 mmol) gave **2a** (422 mg, 89%) as rusty-brown needles. $^1$H NMR (C[$^2$H]$Cl_3$): $\delta$ 1.76 (s, 18 H, $C_6Me_6$), 2.37 (d, $^2J_{HH}$ = 12.3 Hz, 1 H, AB $CH_2$), 4.01 (s, 5 H, $C_5H_5$), 4.12 (m, 2 H, $C_5H_4$, $H_\beta$), 4.14 (m, 1 H, $C_5H_4$, $H_\alpha$), 4.44 (d, $^2J_{HH}$ = 12.3 Hz, 1 H, AB $CH_2$), 4.65 (m, 1 H, $C_5H_4$, $H_\alpha$), 4.66 (s, 3 H, O*Me*), 7.46−7.62 (m, 15 H, $PPh_3$). $^{31}$P{$^1$H} NMR (C[$^2$H]$Cl_3$): $\delta$ −143.0 (sept, $^1J_{PF}$ = 712 Hz, $PF_6^-$), 35.7 (s, $PPh_3$). IR (cm$^{-1}$): $\nu$(CH) 3056 (w), 2923 (w); $\delta_s(CH_3)$ 1385 (m); $\nu$(C−O) 1287 (s); Fc 1095 (m), 1002 (m); $PF_6^-$ 839 (s); $PPh_3$ 491−558 (composed s). Anal. Calcd for $C_{43}H_{47}OF_6P_2ClFeRu$: C, 54.47; H, 4.00. Found: C,

(26) Bennett, M. A.; Huang, T.-N.; Matheson, T. W.; Smith, A. K.; Ittel, S.; Nickerson, W. *Inorg. Synth.* **1982**, *21*, 74.

(27) For general procedure, see: (a) Zelonka, R. A.; Baird, M. C. *Can. J. Chem.* **1972**, *50*, 3063. (b) Bennett, M. A.; Smith, A. K. *J. Chem. Soc., Dalton Trans.* **1974**, 233.

(28) (a) Rosenblum, M.; Brawn, N.; Papenmeier, J.; Applebaum, M. *J. Organomet. Chem.* **1966**, *6*, 173. (b) Rosenblum, M.; Brawn, N.; Ciappenelli, D.; Tancrede, J. *J. Organomet. Chem.* **1970**, *24*, 469.

(29) (a) Sollott, G. P.; Mertwoy, H. E.; Portnoy, S.; Snead, J. L. *J. Org. Chem.* **1963**, *28*, 1090. (b) Kotz, J. C.; Nivert, C. L. *J. Organomet. Chem.* **1973**, *52*, 387.

54.26; H, 4.28. HR LSIMS: *m/z* $[C_{43}H_{47}OPClFeRu]^+$ ($[M - PF_6]^+$), calcd 803.1457, found 803.145.

**[(η⁶-C₆Me₆)Ru(=C(OCH₃)CH₂Fc)(PPh₂Fc)(Cl)] (3a). 3** (353 mg, 0.50 mmol), $NaPF_6$ (84 mg, 0.50 mmol), and FcC≡CH (212 mg, 1.01 mmol) gave **3a** (439 mg, 83%) as a brown solid. $^1$H NMR ($C[^2H]Cl_3$): δ 1.74 (s, 18 H, $C_6Me_6$), 2.21 (d, $^2J_{HH}$ = 12.6 Hz, 1 H, AB $CH_2$), 4.00 (s, 10 H, $C_5H_5$), 4.03 (d, 1 H, AB $CH_2$, identified by selective decoupling), 4.05 (br m, 2 H, $C_5H_4$), 4.10 (m, 2 H, $C_5H_4$), 4.63 (s, 3 H, O*Me*), 4.47−4.82 (br m, 4 H, $C_5H_4$), 7.54−8.02 (br m, 10 H, P*Ph*₂). $^{31}P\{^1H\}$ NMR ($C[^2H]Cl_3$): δ −143.0 (sept, $^1J_{PF}$ = 712 Hz, *P*$F_6^-$), 32.5 (s, *P*$Ph_2$Fc). IR ($cm^{-1}$): ν(CH) 3092 (w), 2922 (w); $\delta_s(CH_3)$ 1386 (m); ν(C−O) 1299, 1262 (s); Fc 1110 (m), 1003 (m); $PF_6^-$ 840 (s); $PPh_2$ 491 (s), 475 (s). Anal. Calcd for $C_{47}H_{51}OF_6P_2ClFe_2Ru$: C, 53.45; H, 4.87; P, 5.87. Found: C, 53.02; H, 4.86; P, 5.74. HR LSIMS: *m/z* $[C_{47}H_{51}OPClFe_2Ru]^+$ ($[M - PF_6]^+$) calcd 911.1123, found 911.114.

**[(η⁶-C₆Me₆)Ru(=C(OCH₃)CH₃)(PPh₂Fc)(Cl)] (3b). 3** (354 mg, 0.50 mmol), $NaPF_6$ (86 mg, 0.51 mmol), and $Me_3SiC{\equiv}CH$ (0.20 mL, 1.4 mmol) gave **3b** (298 mg, 68%) as a rusty-orange solid. $^1$H NMR ($C[^2H]_2Cl_2$): δ 1.87 (s, 18 H, $C_6Me_6$), 2.25 (br s, 3 H, Ru=CC$H_3$), 4.00 (s, 5 H, $C_5H_5$), 4.37 (s, 3 H, O*Me*), 4.55 (br s, 2 H, $C_5H_4$), 4.66 (br s, 2 H, $C_5H_4$), 7.46−7.98 (br m, 10 H, P*Ph*₂). $^{31}P\{^1H\}$ NMR ($C[^2H]_2Cl_2$): δ −143.2 (sept, $^1J_{PF}$ = 711 Hz, *P*$F_6^-$), 32.8 (br s, *P*$Ph_2$Fc). IR ($cm^{-1}$): ν(CH) 3048 (w), 2915 (w); $\delta_s(CH_3)$ 1385 (m); ν(C−O) 1282 (m); Fc 1098 (m), 1001 (m); $PF_6^-$ 839 (s); $PPh_2$ 473−518 (s, composed). HR LSIMS: *m/z* $[C_{37}H_{43}OPClFeRu]^+$ ($[M - PF_6]^+$) calcd 727.1142, found 727.114. The instability of the compound at ambient conditions did not permit us to obtain correct microanalytical results.

**[(η⁶-C₆Me₆)Ru(=C(OCH₃)CH₂Ph)(PPh₂Fc)(Cl)] (3c). 3** (355 mg, 0.50 mmol), $NaPF_6$ (87 mg, 0.52 mmol), and PhC≡CH (0.15 mL, 1.4 mmol) gave **3c** (412 mg, 86%) as a rusty-red microcrystalline solid. $^1$H NMR ($C[^2H]Cl_3$): δ 1.77 (s, 18 H, $C_6Me_6$), 2.51 (d, $^2J_{HH}$ = 13.2 Hz, 1 H, AB $CH_2$), 3.92 (s, 1 H, $C_5H_4$), 3.93 (s, 5 H, $C_5H_5$), 4.45 (s, 1 H, $C_5H_4$), 4.52 (d, $^2J_{HH}$ = 13.2 Hz, 1 H, AB $CH_2$), 4.53 (s, 3 H, O*Me*), 4.66 (s, 1 H, $C_5H_4$), 4.94 (br s, 1 H, $C_5H_4$), 7.01−7.11 (m, 2 H, $CH_2Ph$), 7.21−7.31 (m, 3 H, $CH_2Ph$), 7.55−8.11 (br m, 10 H, P*Ph*₂). $^{31}P\{^1H\}$ NMR ($C[^2H]Cl_3$): δ −143.1 (sept, $^1J_{PF}$ = 712 Hz, *P*$F_6^-$), 32.7 (s, *P*$Ph_2$Fc). IR ($cm^{-1}$): ν(CH) 3057 (w), 2924 (w); $\delta_s(CH_3)$ 1386 (m); ν(C−O) 1301 (s), 1262 (s); Fc 1096 (m), 1003 (m); $PF_6^-$ 839 (s); $PPh_2$ 491 (s), 477 (s). Anal. Calcd for $C_{43}H_{47}OF_6P_2ClFeRu$: C, 54.47; H, 4.00; P, 6.53. Found: C, 54.26; H, 4.09; P, 6.55. HR LSIMS: *m/z* $[C_{43}H_{47}OPClFeRu]^+$ ($[M - PF_6]^+$) calcd 803.1457, found 803.144.

**[(η⁶-C₆Me₆)Ru(=C(OCH₃)CH₂Fc)(Hdpf-*P*)(Cl)] (4a). 4** (375 mg, 0.50 mmol), $NaPF_6$ (86 mg, 0.51 mmol), and FcC≡CH (210 mg, 1.00 mmol) gave **4a** (479 mg, 87%) as brown needles. $^1$H NMR ($C[^2H]_2Cl_2$): δ 1.73 (s, 18 H, $C_6Me_6$), 2.17 (d, $^2J_{HH}$ = 12.8 Hz, 1 H, AB $CH_2$), 4.03 (s, 5 H, $C_5H_5$), 4.04 (d, 1 H, AB $CH_2$, identified by selective decoupling), 4.08 (s, 2 H, $C_5H_4$), 4.16 (s, 2 H, $C_5H_4$), 4.49 (s, 3 H, O*Me*), 4.42−4.82 (br m, 8 H, $C_5H_4$), 7.35−8.15 (br m, 10 H, P*Ph*₂). $^{31}P\{^1H\}$ NMR ($C[^2H]_2Cl_2$): δ −143.3 (sept, $^1J_{PF}$ = 711 Hz, *P*$F_6^-$), 31.8 (br s, *Hdpf*). IR ($cm^{-1}$): ν(CH) 3094 (w), 2925 (w); ν(C=O) 1719, 1677; $\delta_s(CH_3)$ 1386 (m); ν(C−O) 1292, 1270 (s); Fc 1096 (m), 1040 (s), 1002 (m); $PF_6^-$ 841 (s); $PPh_2$ 484 (s). Anal. Calcd for $C_{48}H_{51}O_3F_6P_2ClFe_2Ru$: C, 52.41; H, 4.67; P, 5.63. Found: C, 52.25; H, 4.65; P, 5.55. HR LSIMS: *m/z* $[C_{48}H_{51}O_3PClFe_2Ru]^+$ ($[M - PF_6]^+$) calcd 955.1022, found 955.103.

**[(η⁶-C₆Me₆)Ru(=C(OCH₃)CH₃)(Hdpf-*P*)(Cl)] (4b). 4** (375 mg, 0.50 mmol), $NaPF_6$ (86 mg, 0.51 mmol), and $Me_3SiC{\equiv}CH$ (0.20 mL, 1.4 mmol) gave **4b** (342 mg, 75%) as a rusty-orange solid. $^1$H NMR ($C[^2H]_2Cl_2$): δ 1.85 (s, 18 H, $C_6Me_6$), 2.38 (br s, 3 H, Ru=CC$H_3$), 4.11 (br m, 2 H, $C_5H_4$), 4.33 (s, 2 H, $C_5H_4$), 4.53 (s, 3 H, O*Me*), 4.64 (br s, 1 H, $C_5H_4$), 4.70 (br s, 1 H, $C_5H_4$), 4.84 (br s, 2 H, $C_5H_4$), 7.48−7.82 (br m, 10 H, P*Ph*₂). $^{31}P\{^1H\}$ NMR ($C[^2H]_2Cl_2$): δ −143.2 (sept, $^1J_{PF}$ = 711 Hz, *P*$F_6^-$), 32.3 (br s, *Hdpf*). IR ($cm^{-1}$): ν(CH) 3055 (w), 2918 (w); ν(C=O) 1712 (s), 1671 (s); $\delta_s(CH_3)$ 1385 (m); ν(C−O) 1292 (s); Fc 1096 (m), 1070 (m), 1030 (m); $PF_6^-$ 840 (s); $PPh_2$ 483 (composed m). HR LSIMS: *m/z* $[C_{38}H_{43}O_3PClFeRu]^+$ ($[M - PF_6]^+$) calcd 771.1041, found 771.103. For the instability of this compound at ambient conditions, no relevant microanalytical data could be obtained.

**[(η⁶-C₆Me₆)Ru(=C(OCH₃)CH₂Ph)(Hdpf-*P*)(Cl)] (4c). 4** (374 mg, 0.50 mmol), $NaPF_6$ (86 mg, 0.51 mmol), and PhC≡CH (0.15 mL, 1.4 mmol) gave **4c** (424 mg, 86%) as a rusty-orange solid. $^1$H NMR ($C[^2H]Cl_3$): δ 1.77 (s, 18 H, $C_6Me_6$), 2.52 (d, $^2J_{HH}$ = 13.3 Hz, 1 H, AB $CH_2$), 3.99 (s, 2 H, $C_5H_4$), 4.11 (s, 2 H, $C_5H_4$), 4.52 (s, 3 H, O*Me*), 4.66 (br s, 2 H, $C_5H_4$), 4.73 (s, 2 H, $C_5H_4$), 7.00−7.11 (m, 2 H, $CH_2Ph$), 7.21−7.30 (m, 3 H, $CH_2Ph$), 7.58−8.11 (br m, 10 H, P*Ph*₂). $^{31}P\{^1H\}$ NMR ($C[^2H]Cl_3$): δ −143.1 (sept, $^1J_{PF}$ = 712 Hz, *P*$F_6^-$), 31.9 (s, *Hdpf*). IR ($cm^{-1}$): ν(CH) 3090 (w), 2920 (w); ν(C=O) 1716 (s), 1678 (s); $\delta_s(CH_3)$ 1386 (m); ν(C−O) 1263 (s), 1301 (s); Fc 1097 (m), 1037 (s), 1003 (m); $PF_6^-$ 840 (s); $PPh_2$ 483 (composed s). Anal. Calcd for $C_{44}H_{47}O_3F_6P_2ClFeRu$: C, 53.27; H, 4.77; P, 6.24. Found: C, 52.88; H, 4.86; P, 6.24. HR LSIMS: *m/z* $[C_{44}H_{47}O_3PClFeRu]^+$ ($[M - PF_6]^+$) calcd 847.1356, found 847.135.

**Structure Determination.** Thin, plate-like and fragile crystals of **4a**·$CH_2Cl_2$ were grown by gas-phase diffusion of pentane into a dichloromethane solution of **4a**. They were isolated by decantation and mounted on a glass fiber by epoxy cement. The diffractions were measured at 296(1) K on an Enraf-Nonius CAD 4-MACH III diffractometer using graphite-monochromated Mo Kα radiation (λ = 0.710 73 Å) and θ−2θ scan. Intensities were collected at ψ-angles with the lowest absorption predicted. No further correction for absorption was made. The cell parameters were determined by least-squares from 25 centered diffractions with $12.0 \le \theta \le 12.8°$.

The structure was solved by direct methods (SIR92[30]), followed by consecutive Fourier syntheses and refined by full-matrix least-squares on $F^2$ (SHELX93[31]). Non-hydrogen atoms were refined anisotropically, except those of the solvate dichloromethane. Aromatic (ferrocenyl, phenyl), methylene ($FcCH_2$, $CH_2Cl_2$), and methyl ($C_6Me_6$, $OCH_3$) hydrogens were fixed in theoretical positions to fit aromatic C−H (0.93 Å), ideal methylene group (C−H 0.97 Å), or electron density maxima (C−H 0.96 Å), respectively, with $U_{iso}(H) = 1.2\ U_{eq}(C)$. The carboxylic hydrogen was identified on a difference electron density map and refined. The hexafluorophosphate anion and dichloromethane are partly disordered due to high symmetry or weak secondary bonding, respectively. The small crystal volume and the presence of partly disordered moieties are responsible for the higher values of the *R* indices.

**Acknowledgment.** This work was supported by the Grant Agency of Charles University, the Grant Agency of Czech Republic, and the CNRS. P.Š. gratefully acknowledges a fellowship in Rennes.

**Supporting Information Available:** Tables of crystallographic data, calculated and refined positional parameters, anisotropic thermal parameters, and intramolecular distances and angles and a packing diagram of **4a**·$CH_2Cl_2$ (14 pages). Ordering information is given on any current masthead page.

OM970478K

(30) Altomare, A.; Burla, M. C.; Camalli, M.; Cascarano, G.; Giacovazzo, C.; Guagliardi, A.; Polidori, G. *J. Appl. Crystallogr.* **1994**, *27*, 435.

(31) Sheldrick, G. M. *SHELXL93. Program for Crystal Structure Refinement from Diffraction Data*; University of Göttingen: Göttingen, Germany, 1993.